Structural Characterization and Mechanical Behavior of Metallocenic Copolymers of Ethylene and 5,7-Dimethylocta-1,6-diene

María L. Cerrada,[1] Rosario Benavente,[1] José M. Pereña,[1] Ernesto Pérez,[1] Jorge Moniz-Santos,[2] M. Rosário Ribeiro[2]*

[1]Instituto de Ciencia y Tecnología de Polímeros (CSIC), C/ Juan de la Cierva 3, 28006 Madrid, Spain
[2]Grupo de Estudos de Catálise Heterogénea, Instituto Superior Técnico, Av. Rovisco País, 1049-001 Lisboa, Portugal

Summary: The relationships between structure and mechanical properties have been established in several copolymers of ethylene and 5,7-dimethylocta-1,6-diene synthesized by a metallocene catalyst. A dependence with composition and polymerization temperature has been found for different structural and mechanical parameters. The branches cannot be incorporated into the orthorhombic crystal lattice and, consequently, structural parameters such as crystallinity and crystal size are considerably affected as 5,7-dimethylocta-1,6-diene content increases in the copolymer. These structural changes influence significantly the rigidity of the copolymers and a decrease of this parameter, determined from either storage modulus or microhardness, with increasing 5,7-dimethylocta-1,6-diene molar fraction is found. The location of the different viscoelastic relaxations is also strongly dependent on composition.

Keywords: crystallinity; ethylene-5,7-dimethylocta-1,6-diene copolymers; metallocene catalysts; microhardness; relaxation

Introduction

Many efforts have been made to use metallocene catalysts for the copolymerization of olefins with functional monomers since their advent. However, a strong deactivation of the catalyst by the functional monomer is observed. Different procedures have been developed in order to defeat this problem. They include the use of vinyl monomers bearing functional groups that are distant to the double bond,[1] or sterically hindered,[1-3] or protected by a pre-complexation reaction.[4-6]

Another approach to the production of functionalized polyolefins less harmful to catalyst activity involves the copolymerization of olefins with pro-functional monomers followed by

 DOI: 10.1002/masy.200450928

the chemical modification of these pre-formed polymers. Boranes and dienes[7-13] are common examples. Concerning the second mentioned choice, unsaturated polyolefins are obtained by copolymerization of α–olefins with non-conjugated dienes. They present pendent olefin unsaturations that can be easily reacted with different functional groups. Reported methods include bromination, epoxidation, radical addition and hydrosilylation.[11-13] These polymers are, therefore, useful intermediates in the production of side functional polyolefins, which can then act as interfacial modifiers to enhance adhesion and compatibility of polyolefins with other polymers, fillers or even fibers.

We have, recently, obtained polyethylenes with high incorporations of 5,7-dimethylocta-1,6-diene, labelled as DMO. The structure of this diene helps preventing side-reactions like cyclization and crosslinking.[14] Therefore, the objective of this work is to characterize the structure in the solid state of these precursors of functionalized polyolefins, that are a series of copolymers of ethylene and DMO in a wide range of compositions. In addition to the previously mentioned structural characterization of these copolymers, named as CEDMO, the analysis of their mechanical behavior by means of either dynamic mechanical or microhardness measurements is presented.

Experimental

Polymerization reactions were carried out as follows: toluene, ethylene and DMO comonomer were charged into the reactor. A constrained geometry metallocene catalyst [14] (CGC) (η_5-C_5Me_4)$SiMe_2$(N*tert*Bu)$TiCl_2$ was pre-contacted with methylaluminoxane (MAO) for 15 min prior introduction of this pre-activated catalyst into the reactor. After 1 h, polymerization was stopped and the polymers were carefully washed and dried preceding to characterization. Two different polymerization temperatures were utilized: 25°C and 60°C, to learn the effect of this variable on the final properties. Several CEDMO copolymers with different comonomer content, ranging from 1.4 to 10 mol % in DMO, were obtained, as seen in Table 1. The DMO molar fraction was estimated from 1H NMR spectra performed in 1,1,2,2-tetrachloroethane at 107°C with a Bruker MSL 300P spectrometer.

The different CEDMO copolymers and the corresponding homopolymers were prepared as films by compression molding in a Collin press at 140°C at a pressure of 1.5 MPa for 5 min and a further quenching within Teflon plates cooled with water.

Wide and small-angle X-ray diffraction patterns, WAXS and SAXS respectively, were recorded in the transmission mode at room temperature employing synchrotron radiation (λ= 0.150 nm) in the beamline A2 at HASYLAB (Hamburg, Germany). Two linear position-sensitive detectors were used. The SAXS one, at a distance of 235 cm from the sample, was calibrated with the different orders of the long spacing of rat-tail cornea (L = 65 nm). It was found to cover a spacings range from 5 to 55 nm. The WAXS detector, covering a 2θ range from about 10 to 30 degrees, was calibrated with the different diffractions of crystalline PET.

Table 1. DMO composition and sample characteristics. Experimental conditions with CGC catalyst for polymerization at 25 °C: [Ti] = $7\text{-}10 \cdot 10^{-5}$ mol/L, Al/Ti = 1000, P_{et} = 3.4 bar and for polymerization at 60 °C with CGC catalyst: [Ti] = $3\text{-}6 \cdot 10^{-5}$ mol/L, Al/Ti = 1000, P_{et} = 1.0 bar

Sample	DMO content (mol-%)	M_w/M_n	M_w (10^3 g · mol^{-1})
Polymerization Temperature: 25°C			
25HDPE	0.0	3.1	149
25CEDMO1	1.4	2.0	79
25CEDMO2	4.0	2.3	75
25CEDMO3	5.8	6.3	74
Polymerization Temperature: 60°C			
60HDPE	0	2.3	57
60CEDMO1	2	2.8	56
60CEDMO2	4.4	7.5	25
60CEDMO3	7.8	n. d.	n. d.
60CEDMO4	10	n. d.	n. d.

Calorimetric analyses were carried out in a Perkin-Elmer DSC7 calorimeter, connected to a cooling system and calibrated with different standards. The sample weights ranged from 5 to 7.5 mg. A temperature range from -70°C to 150°C has been studied with a heating rate of 10°C min^{-1}. For crystallinity determinations, a value of 290 J g^{-1} has been taken as the enthalpy of fusion of a perfectly crystalline material.[15]

Viscoelastic properties were measured with a Polymer Laboratories MK II dynamic mechanical thermal analyzer working in the tensile mode. The real (E′) and imaginary (E″)

components of the complex modulus and the loss tangent (tan δ) of each sample were determined at 1, 3, 10 and 30 Hz, over a temperature range from -150 to 150°C, at a heating rate of 1.5°C min^{-1}.

A Vickers indentor attached to a Leitz microhardness tester was used to carry out microindentation measurements undertaken at 23°C. A contact load of 0.98 N and a contact time of 25 s were employed. Microhardness, MH, values (in MPa) were calculated according to the relationship:

$$MH = 2 \sin 68^{\circ} P / d^{2} \qquad [1]$$

where P (in N) is the contact load and d (in mm) is the diagonal length of the projected indentation area.

Results and Discussion

Crystalline structure and thermal properties

Polyethylene crystallizes in an orthorhombic lattice under usual conditions. This crystalline cell is characterized by two main diffraction peaks: the (110) and the (200). It is known that in general, the alkyl branches cannot enter into the polyethylene crystal lattice, although the methyl branches are included in the crystalline cell at a substantial degree.[16,17] The DMO comonomer units copolymerized here with ethylene are bulkier than common alkyl ones and, therefore, the capability of being incorporated into the crystalline lattice does not practically exist and the hindrance imposed for the PE crystallization is expected to be high. Consequently, the presence of the DMO comonomer leads to a significant decrease of the (110) and (200) diffraction intensities and, accordingly, the crystallinity in the copolymers diminishes as DMO content increases, as depicted in Figure 1. In addition, a shift of the positions of the maxima to lower angles and a broadening of crystalline diffractions are observed. This broadening indicates a decrease in the crystallite size with the increase of DMO content. It is important to note that all of the samples analyzed display a clear long spacing, L, as listed in Table 2, which is attributed to the presence of lamellar crystals though some of the specimens are practically amorphous, as observed from WAXS patterns. In these cases, for high DMO contents, bundles of crystallites are expected. Moreover, long spacing strongly depends upon both comonomer composition and polymerization temperature. On the one hand, a decrease of long spacing with the increase of DMO content is observed and, on

the other hand, larger long spacings are found in the copolymers synthesized at 25°C due to their higher molecular weight.

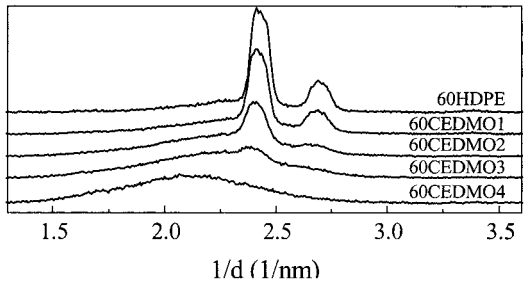

Figure 1. WAXS patterns of the samples polymerized at 60°C

The crystallite thickness, l_c, has been determined from the long spacing and the WAXS crystallinity by assuming a simple two-phase model. This method will be only applicable for those cases where uniform lamellae stacks are present. Anyway, decrease of the crystallite thickness values is observed as DMO content is increased in the copolymers (Table 2).

Table 2. Melting temperatures (T_m), enthalpies of melting (ΔH_m), crystallinities estimated from either D.S.C. or WAXS data (f_c^{DSC} and f_c^{WAXS}), long spacings (L), crystal thickness (l_c), relaxation temperatures (E'' basis, at 3 Hz), storage modulus (E' at 25°C and at 3Hz) and microhardness of the different specimens

Sample	T_m (°C)	ΔH_m (J g^{-1})	f_c^{DSC}	f_c^{WAXS}	L (nm)	l_c (nm)	T_γ (°C)	T_β (°C)	T_α (°C)	E'_{25} (MPa)	MH (MPa)
Polymerization Temperature: 25°C											
25HDPE	132	194	0.67	0.64	27.8	17.8	-118	-	54	1432	37
25CEDMO1	124	151	0.52	0.55	15.2	8.4	-119	-22	42	605	17
25CEDMO2	91	81	0.28	0.26	12.2	3.2	-134	-28	12	90	8
25CEDMO3	62	41	0.14	0.05	11.4	0.6	-126	-6	-	21	4
Polymerization Temperature: 60°C											
60HDPE	132	209	0.72	0.72	20.1	14.5	-118	-	48	1670	38
60CEDMO1	126	168	0.58	0.60	17.7	10.6	-118	-15	45	845	23
60CEDMO2	107	84	0.29	0.35	11.6	4.1	-133	-16	18	100	8
60CEDMO3	69	41	0.14	0.10	10.3	1.0	-134	-26	-5	12	3
60CEDMO4	61	12	0.04	-	10.2	-	-129	-12	-	3.7	1

The d.s.c. traces for the different samples support the X ray diffraction results just mentioned, as represented in Figure 2. A depression of the melting temperature (T_m) is observed, as

expected, as DMO content increases owing to the smaller crystallite sizes (assuming that Tm only depends on the composition of the melt). In addition, a broadening of the melting region is also found in the copolymers with higher DMO compositions. On the other hand, the melting enthalpy is also significantly reduced with increasing DMO content in the copolymer.

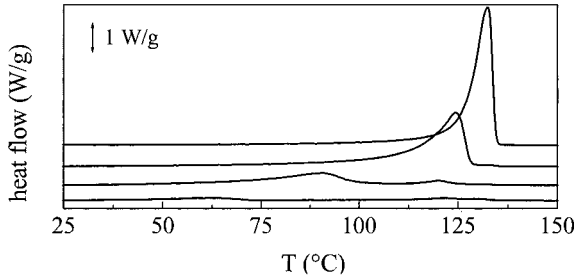

Figure 2. D.s.c. melting curves corresponding to the specimens polymerized at 25°C. From top to bottom: 25HDPE, 25CEDMO1, 25CEDMO2, 25CEDMO3

Moreover, at a given comonomer content, the distortion on the crystallites is larger in the current copolymers than in cases where the branches are 1-hexene, 1-octene[18] or even longer alkyl lateral chains,[19] as seen in Figure 3.

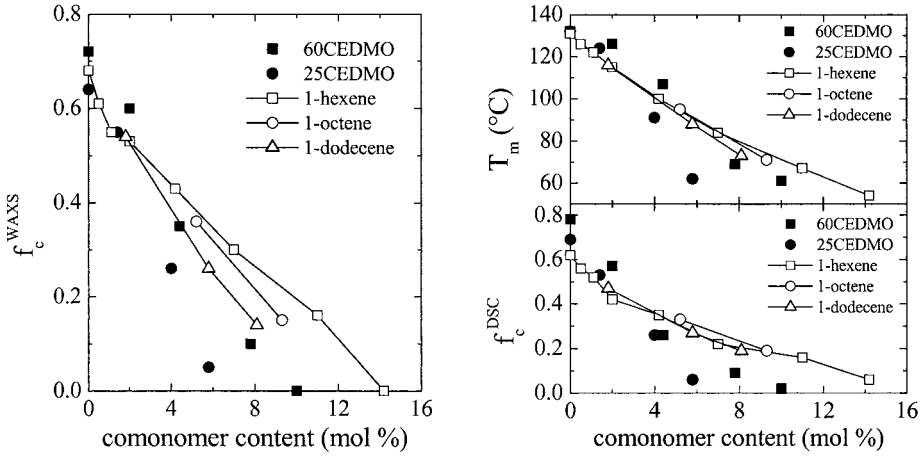

Figure 3. Dependence of crystallinity estimated by WAXS experiments (left picture), melting temperature and crystallinity estimated by DSC measurements (right picture: upper and lower plot, respectively) with comonomer content of the different CEDMO specimens under study and other ethylene copolymer samples

This feature may be attributed to the dimethyl substitutions within the branches and, accordingly, to a higher global volume of the comonomer unit. Therefore, similar values of crystallinity, melting temperature and long spacing are observed compared to those obtained for 1-hexene, 1-octene or 1-octadecene copolymers but in the current ethylene-DMO specimens those values are shown at lower comonomer incorporation.

Viscoelastic behavior and microhardness measurements

The viscoelastic behavior of polyethylene is strongly influenced by variables characteristic of the crystalline regions, such as crystallinity and lamellar thickness.[20] Therefore, a decrease of the storage modulus is seen as DMO content increases and, accordingly, crystallinity and crystal size diminish, this feature being related to the reduction of rigidity (Figure 4).

Such a diminution in stiffness with DMO composition has also been found in the microhardness values, as shown in Figure 4. On the other hand, it seems that the MH values are slightly higher in the copolymers obtained at 60°C at a similar comonomer content because of their lower molecular weights.

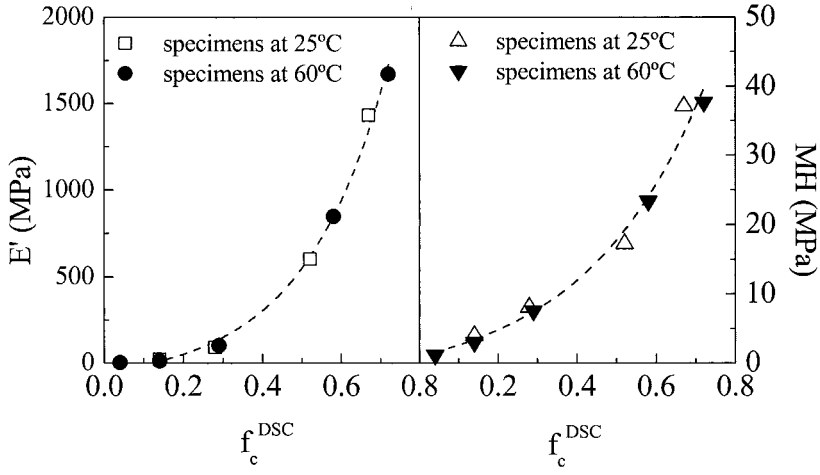

Figure 4. Dependence of E′ (left plot) and MH (right plot) on crystallinity for the different specimens

MH measures mostly the resistance of the material to plastic deformation. A direct correlation is commonly found between the elastic modulus (here represented by storage modulus, E′) and MH and the following empirical equation has been proposed:[21]

$$MH = a \cdot E^b \qquad [2]$$

where a and b are constants. As seen in Figure 4, both magnitudes, storage modulus and MH, display an analogous variation with crystallinity for the two copolymerization temperatures corroborating the mentioned direct relationship between these two mechanical parameters for these CEDMO copolymers.

Concerning the viscoelastic response several relaxation processes are observed depending upon composition: γ, β and α in order of increasing temperatures.

The γ relaxation in polyethylene was firstly attributed to crankshaft movements of polymethylenic chains. Figure 5 displays a shift to lower temperatures of the γ peak as the DMO content rises in the copolymers since this process is associated to the amorphous phase and there is a higher mobility in the amorphous regions, as DMO incorporation increases.

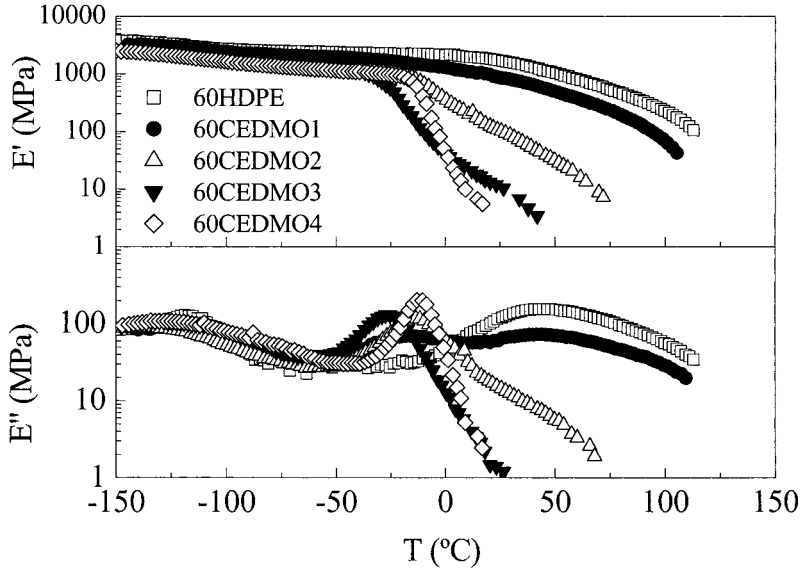

Figure 5. Temperature dependence of the two components to the complex modulus for the specimens polymerized at 60°C

The β relaxation process in the CEDMO copolymers is also moved to lower temperatures and its intensity becomes higher as comonomer molar fraction increases. However, a shift to higher temperatures is observed in the copolymers with the highest comonomer content either that prepared at 25°C or at 60°C. This feature in those two copolymers with the highest DMO molar fractions seems to point that other additional effect is taking place. A certain degree of crosslinking might be possible for those highest DMO contents.

The α relaxation in polyethylene has been associated to vibrational and reorientational motions within the crystallites. The location of the α relaxation depends strongly on the comonomer content. Thus, this process is only clearly observed in the homopolymers and in copolymers with low DMO incorporations. For higher contents, the lower crystallinity joined to the smaller and more imperfect crystallites lead to a decrease of the intensity and a shift to lower temperatures of this α relaxation and an overlap with the β process is observed. A good linear relationship is found between the location of this relaxation, T_α, and the crystallinity (Figure 6). However, its correlation with the most probable crystal thickness, l_c, is not linear (Figure 6). A very similar non-linear variation has been reported before[22,23] for other ethylene copolymers.

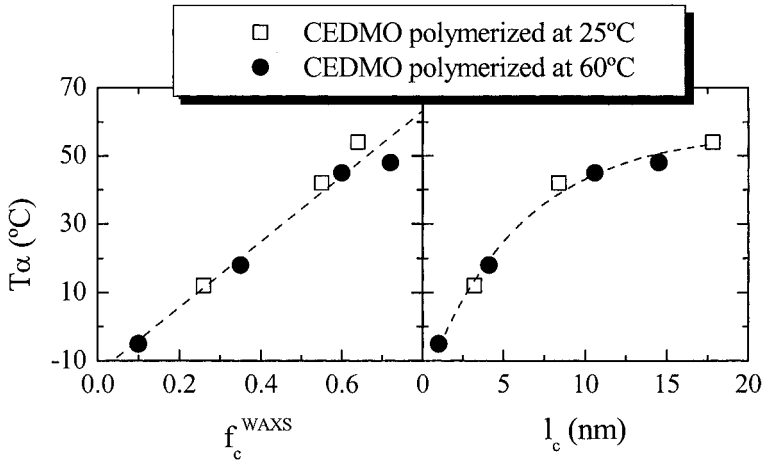

Figure 6. Variation of location of α relaxation, T_α, with crystallinity (left plot) and crystal thickness (right plot) for the different specimens

Conclusions

The most important factor affecting the structure and properties of these CEDMO copolymers is, evidently, the comonomer content and its influence on crystallinity and crystallite thickness. The distortion on the crystallites is larger in the current copolymers than in cases where the branches are common alkyl lateral chains. Higher crystallinities and smaller crystal sizes have been found in copolymers synthesized at 60°C at a similar comonomer content, probably due to their lower molecular weights. A relationship has been found between storage modulus and microhardness, showing a similar dependence with structural parameters. A shift to lower temperatures is generally found for the γ and β relaxations as DMO content increases. Finally, the α relaxation is also moved to lower temperatures as crystallinity and crystal thickness decrease and a linear dependence is found between its location and the former parameter.

Acknowledgements

The financial support of the Comunidad Autónoma de Madrid, Ministerio de Ciencia y Tecnología, Comisiones Mixtas CSIC/ICCTI and CSCI/CNR, and Fundação para a Ciência e Tecnologia (Projects 07G/0038/2000, MAT2001-2321, 2002PT0001-Proc. 423, 2003IT0006 and POCTI/CTM/41408/2001, respectively) is gratefully acknowledged. The IHP Programme "Access to Research Infrastructures" of the European Commission has supported the synchrotron work in the polymer line of Hasylab at DESY, Hamburg (Contract HPRI-CT-1999-00040). We thank the collaboration of the Hasylab personnel, and specially Dr. S. Funari, responsible of the polymer beamline.

[1] M. R. Kesti, G. W. Coates, R. M. Waymouth, *J. Am. Chem. Soc.* **1992**, *114*, 9679.
[2] R. Goretzki, G. Fink, *Macromol.Rapid Commun.* **1998**, *19*, 511.
[3] C. Wilen, H. Luttikhedde, T. Hjertberg, J. H. Nasman, *Macromolecules* **1996**, *29*, 8569.
[4] P. Aaltonen, G. Fink, B. Lofgren, J. Seppala, *Macromolecules* **1996**, *29*, 5255.
[5] R. Goretzki, G. Fink, *Macromol. Chem. Phys.* **1999**, *200*, 881.
[6] J. M. Santos, M. R. Ribeiro, M. F. Portela, S.G. Pereira, T. G. Nunes, A. Deffieux, *Macromol. Chem. Phys.* **2001**, *202*, 2195.
[7] W. Kaminsky, D. Arrowsmith, H.R. Winkelbach, *Polym. Bull.* **1996**, *36*, 577.
[8] M. Dolatkhani, H. Cramail, A. Deffieux, *Macromol. Chem. Phys.* **1996**, *197*, 2481.
[9] P. Pietikäinen, P. Stark, J.V. Seppälä, *J. Polym. Sci., Part A: Polym. Chem.* **1999**, *37*, 2379.
[10] P. Pietikäinen, J.V. Seppälä, L. Ahjopalo, L-O Pietilä, *Eur. Polym. J.* **2000**, *36*, 183.
[11] M. Hackmann, T. Repo, G. Jany, B. Rieger, *Macromol. Chem. Phys.* **1998**, *199*, 1511.

[12] J. Suzuki, Y. Kino, T. Uozumi, T. Sano, T. Teranishi, J. Jin, K. Soga, T. Shiono, *J. Appl. Pol. Sci.* **1999**, *72*, 103.
[13] T. Uozumi, G.L. Tian, C.H. Ahn, J.Z. Jin, S. Tsubaki, T. Sano, K. Soga, *J. Polym. Sci. Part A: Polym. Chem.* **2000**, *38*, 1844.
[14] J. M. Santos, M. R. Ribeiro, M. F. Portela, H. Cramail, A. Deffieux., A. Antiñolo, A. Otero, S. Prashar, *Macromol. Chem. Phys.* **2002**, *203*, 139.
[15] B. Wunderlich, "*Macromolecular Physics*", Academic Press, New York **1980**, vol. *3*, p. 42.
[16] E. Pérez, D. L. VanderHart, *J. Polym. Sci., Part B: Polym. Phys.* **1987**, *25*, 1637.
[17] R. Alamo, R. Domszy, L Manderkern, *J. Phys. Chem.* **1984**, *88*, 6587.
[18] M. L. Cerrada, R. Benavente, E. Pérez, *J. Mater. Res.* **2001**, *16*, 1103.
[19] R. Benavente, E. Pérez, R. Quijada, *J. Polym. Sci., Part B: Polym. Phys.* **2001**, *39*, 277.
[20] I.M. Ward, "*Mechanical Properties of Solids Polymers*", 2nd edition, J. Wiley and Sons. Chichester, **1985**.
[21] F. J. Baltá-Calleja, *Adv. Polym. Sci.* **1985**, *66*, 117.
[22] R. Popli, M. Glotin, l. Mandelkern, R. S. Benson, *J. Polym. Sci., Part B: Polym. Phys.* **1984**, *22*, 407.
[23] J. M. Martínez-Burgos, R. Benavente, E. Pérez, M. L. Cerrada. *J. Polym. Sci., Part B: Polym. Phys.* **2003**, *41*, 1244.